Raman scattering study of ammonia up to 75 GPa: Evidence for bond symmetrization at 60 GPa

M. Gauthier, Ph. Pruzan, J. C. Chervin, and J. M. Besson
Physique des Milieux Condenses, Tour 13, 4eme Etage, Université Pierre et Marie Curie, 4 place Jussieu, 75230 Paris Cédex 05, France
(Received 9 March 1987)

Results from a Raman scattering study of ammonia up to 75 GPa in a diamond-anvil cell are reported. Both internal and external modes were investigated up to 30 GPa and internal modes were further examined up to 75 GPa. The results show a phase transformation at 14 GPa and point to another one at 60 GPa, the latter transformation leading very likely to a symmetric H-bonded solid.

I. INTRODUCTION

The aim of this work is twofold. Firstly, it is to investigate the phase diagram of ammonia above 6 GPa, and secondly, to know more about the behavior of a weakly H-bonded solid under several tens of GPa.

Until recently, the high-pressure forms of solid ammonia were not known. Raman scattering, x-ray, neutron-diffraction, volume, and ultrasonic measurements allowed the study of the domain at 6 GPa from 170–295 K.[1–5] Several scattering techniques have recently been applied to the study of the dynamical properties of NH_3 below 1 GPa.[4,6–11] As shown in Fig. 1, four solid forms were known until now.

The effect of very high pressure is a strong decrease of the intermolecular distances. This deeply modifies the interatomic bonds of the molecule. For example, it was shown in the case of ice that pressure is a physical way to strengthen the H bond H $\cdots$ O.[12–15] Such a strengthening is at the expense of the O—H covalent bond.[16] In ice, such effects may cause deep changes in the nature of the intermolecular H bond, which should become at least partly ionic around 42 GPa when symmetrization of the H bond is reached.[15,17,18] In that respect NH_3 is an interesting test since it is a simple example of a weakly H-bonded molecular solid. Moreover, its properties are of interest for solid-state physics, and also for astrophysical modeling. Among the different probes quoted above, Raman scattering is one of the most appropriate tools to investigate this kind of problem. Actually, the Raman spectrum contains a great deal of information about symmetry properties of the sample under investigation and, although unpolarized spectra are obtained, this technique is well suited to studies in the diamond-anvil cell (DAC).

We report here Raman scattering results on NH_3 at room temperature in the DAC up to 75 GPa. Using group-theoretical analysis, these data will be discussed by considering the known symmetry properties of NH_3 at low pressure as well as structural symmetry arguments and specific features of the H bond. Accordingly, we show that our data are sufficient to propose a restricted set of possible structures for solid NH_3 at 14 and 60 GPa. Emphasis is given to the fact that compression of ammonia under several tens of GPa progressively leads to a solid which loses its molecular character.

II. EXPERIMENT

Two different DAC's were used. Up to 30 GPa we used a DAC which is similar to that designed by Bloch and Piermarini.[19] The diameter of the diamond culet was 650 μm, which provides a rather large sample space. The gasket hole was about 300 μm and the original thickness 80 μm. Above 30 GPa and up to 75 GPa the cell used was similar to that of Mao and Bell[19] with beveled-diamond anvils and a central flat diameter around 250 μm. The hole in the gasket was about 50 μm and 50 μm in thickness. The sample space was filled by condensing liquid ammonia (Air Liquide, 99.95% purity) using an *ad hoc* gas-tight chamber capping the cell. Closure of the system encloses the NH_3 sample under a pressure around 5 GPa. Pressure was measured using the shift of 3000-ppm Cr^{3+} ruby chips initially placed in the sample space along the Mao-Bell pressure scale.[20] Raman spectra were recorded with a T800 Coderg triple monochromator with a cooled photomultiplier detector and a photon-counting system. The instrumental resolution was 5 cm^{-1}. We used a forward-scattering geometry (0°); the laser beam (400 mW, 488.0 nm) from an argon-ion laser was focused down to about 10 μm on the sample.

III. RESULTS

The Raman spectra of ammonia solid phase I were extensively studied at atmospheric pressure and low temperature.[21] The internal modes, also investigated in the liquid phase,[22,23] are mainly characterized by a strong scattering around 3300 cm^{-1} where three overlapping bands exist [Fig. 2(a)], which are assigned in order of increasing frequencies to ν_1 the symmetric stretching mode, $2\nu_4$ the overtone of the bending mode ν_4, and ν_3 the antisymmetric stretching mode. It is generally ac-

cepted that the two bands ν_1 and $2\nu_4$ are in Fermi resonance. The two bending modes ν_2 and ν_4 are observed, respectively, around 1060 and 1640 cm^{-1} in the solid state. External modes of phase I were reported at atmospheric pressure[21,24,25] and under pressure.[1,6,7] Details on the mode assignments are given in Sec. IV A.

A. Phase III

At room temperature and above 1.2 GPa, NH_3 crystallizes in a cubic phase $Fm3m$ (O_h^5). Since the site symmetry is $m3m$ (O_h),[2,5] this phase is orientationally disordered (see Sec. IV A).

With an optical high-pressure vessel we already studied the Raman spectra of this phase close to the melting line.[7] The strong scattering region around 3300 cm^{-1}

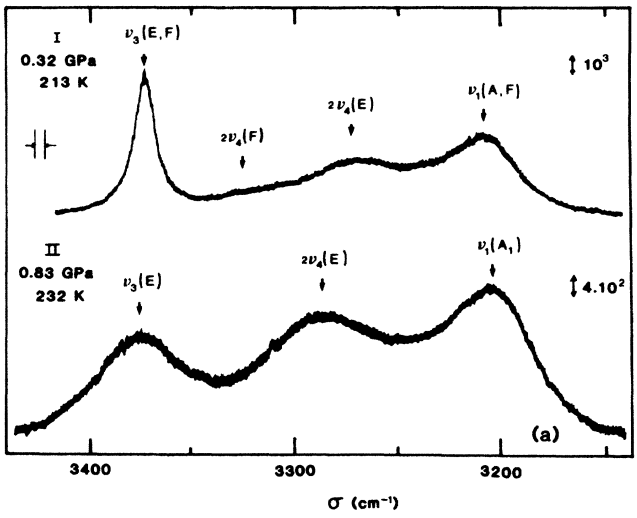

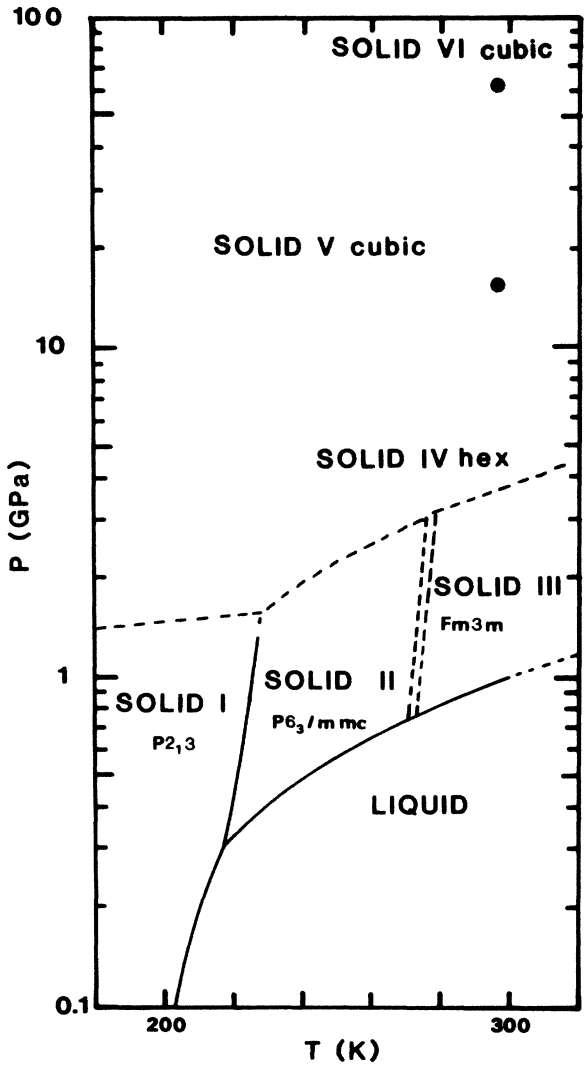

FIG. 1. Phase diagram of ammonia, pressure in log scale vs T. Solid line according to Ref. 3; dashed line according to Ref. 5; ●, above 6 GPa at 295 K, this work. According to this study, solid phase IV is $P6_3/mmc$ (site symmetry $3m$), solid phase V is $I\bar{4}3m$ (site symmetry $3m$), and solid phase VI may be $Pm3m$ (site symmetry $m3m$ for N atoms and $4/mmm$ for H atoms).

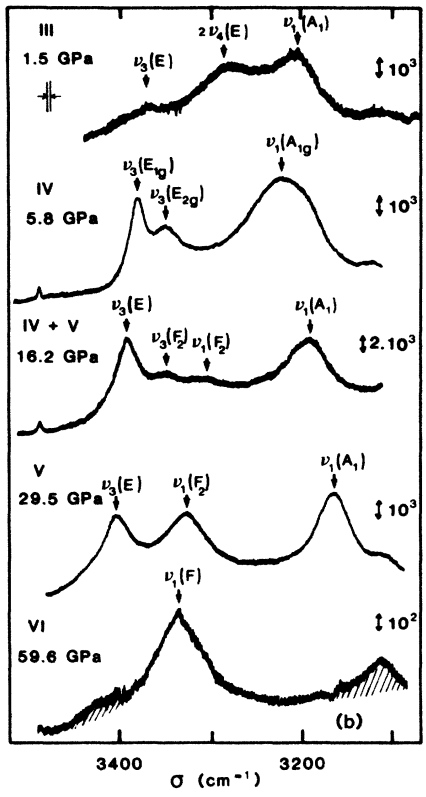

FIG. 2. Typical internal spectra of the NH_3 solid phases. Intensity in counts/s, wave number is in cm^{-1}. Spectral resolution is 5 cm^{-1}. (a) Internal spectra of NH_3 solid phase I at 0.32 GPa and 213 K, and NH_3 solid phase II at 0.83 GPa and 232 K. Assignments of the peaks are provided according to Tables I and II. (b) From top to bottom, internal spectrum of NH_3 solid phases III, IV, V, and VI at 295 K. Assignments of the peaks are provided according to Tables III–VI. For clarity, the notation ν_1 (F) is kept for the spectra of solid phase VI. Peaks from optical system luminescence are shaded.

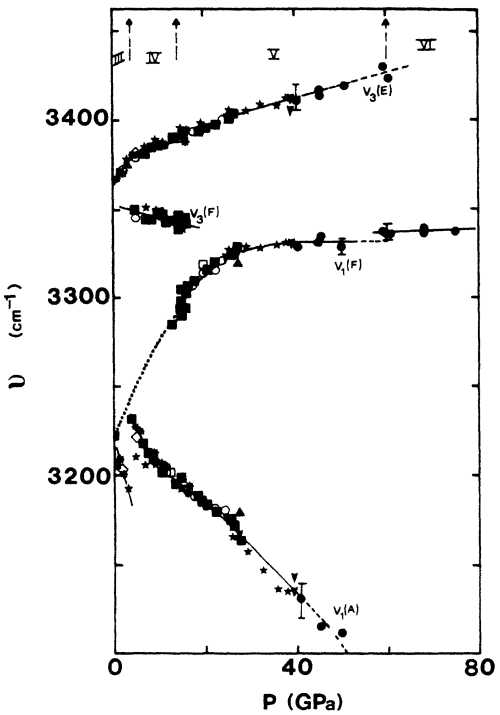

FIG. 3. Symmetric and antisymmetric stretching mode frequencies of NH_3 and their components vs pressure. Symbols indicate different samples; solid lines, experimental curves; dotted line, extrapolation of ν_1 (F) at low pressure; dashed lines, rough behavior of ν_1 (A) and ν_3 (E) above 40 GPa. Below 30 GPa the uncertainty of ν is around ± 2 cm^{-1}, above 30 GPa the uncertainty for ν_1 (A) and ν_3 (E) may reach ± 10 cm^{-1} and ± 5 cm^{-1} for ν_1 (F); error bars are given at 40 GPa. On the top, arrows give transition pressures. For clarity, notations are those used for NH_3 solid phase I.

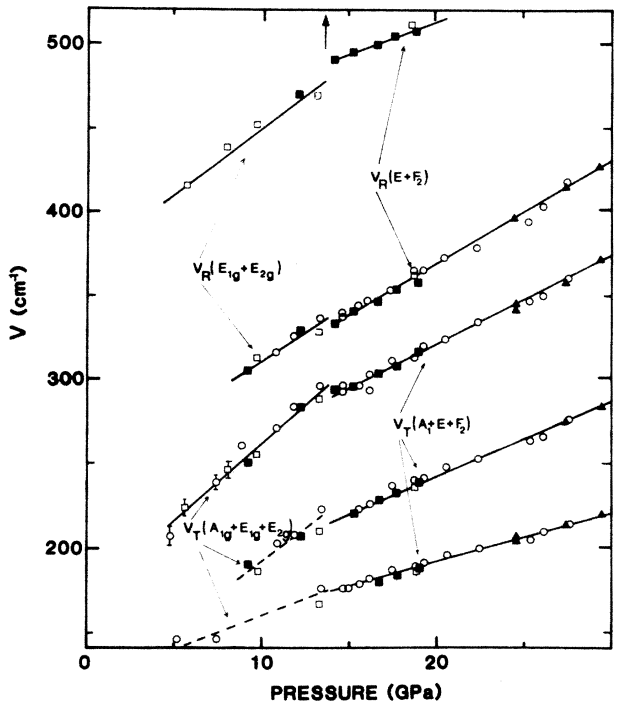

FIG. 4. Frequencies of the lattice modes of solid NH_3 phases IV and V as a function of pressure. Symbols indicate different samples; solid lines, experimental curves; dashed lines, estimated behavior; arrow on the top, position of the transition IV-V. Assignments are given according Tables IV and V. Error bars, ± 5 cm^{-1} around 6 GPa, ± 2 cm^{-1} above 10 GPa.

and at 1.5 GPa is shown in Fig. 2(b); it is very similar to that of the liquid phase. The three broad peaks are assigned from the lower frequencies, to ν_1, $2\nu_4$, and ν_3. Deconvolution shows that the envelope consists of five overlapping bands. The symmetric stretching frequency ν_1 is observed to decrease with pressure, whereas the antisymmetric stretching frequency ν_3 increases (see Fig. 3 and Sec. IV B). We did not observe Raman-active lattice modes in accordance with the symmetry properties of phase III (see Sec. IV A). Above 2 GPa, strong Raman-active librational modes are observed. This indicates that in this range the phase transition line II-III is not the dotted straight line given in Fig. 1, although it has been proposed in a recent x-ray investigation.[5]

B. Phase IV

At room temperature the transformation which occurs at around 3.8 GPa is easily observed, owing to the birefringent character of the new phase.[1] X-ray data[5] show that phase IV has an hexagonal symmetry with a c/a ratio, at 3.8 GPa, slightly above the ideal value of 1.633 for a compact structure. This ratio decreases with pressure to 1.633 at 6 GPa. Compared to phase III the shape of the vibron modes is deeply changed [Fig. 2(b)]. Three peaks are resolved, one fairly broad in the ν_1 region and two in the ν_3 range. Deconvolution shows that the spectrum consists of at least five overlapping bands, which for clarity are not given in Fig. 2(b).

At the III-IV transition the frequency ν_1 experiences a positive 35-cm^{-1} jump, then decreases upon further compression (Fig. 3). Apart from the newly resolved component of ν_3, which decreases with pressure, no change can be observed on the variation of ν_3 versus p, which increases upon further compression.

Five external Raman-active modes were observed in solid phase IV. Frequencies ν versus pressure p are plotted in Fig. 4. Grüneisen parameters are found to be between 1.9 and 1.2 for translational modes and around 0.65 for rotational modes. Widths are from the lower frequency mode, 10, 10, 40, 20, and 50 cm^{-1}, respectively. It is interesting to note that these modes may be clearly observed only above 6 GPa.

C. Phase V

Around 14 GPa the following points indicate the occurrence of a new phase: (i) The form of the spectrum around 3300 cm^{-1} begins to modify showing the occurrence of a new mode [see Fig. 2(b)]; (ii) we can detect slight changes in the variations ν_1 and ν_3 versus p (Fig. 3); and (iii) plots of the three external higher frequencies versus pressure exhibit jumps or a change in the slope $d\nu/dp$ (see Fig. 4). These small changes suggest that the

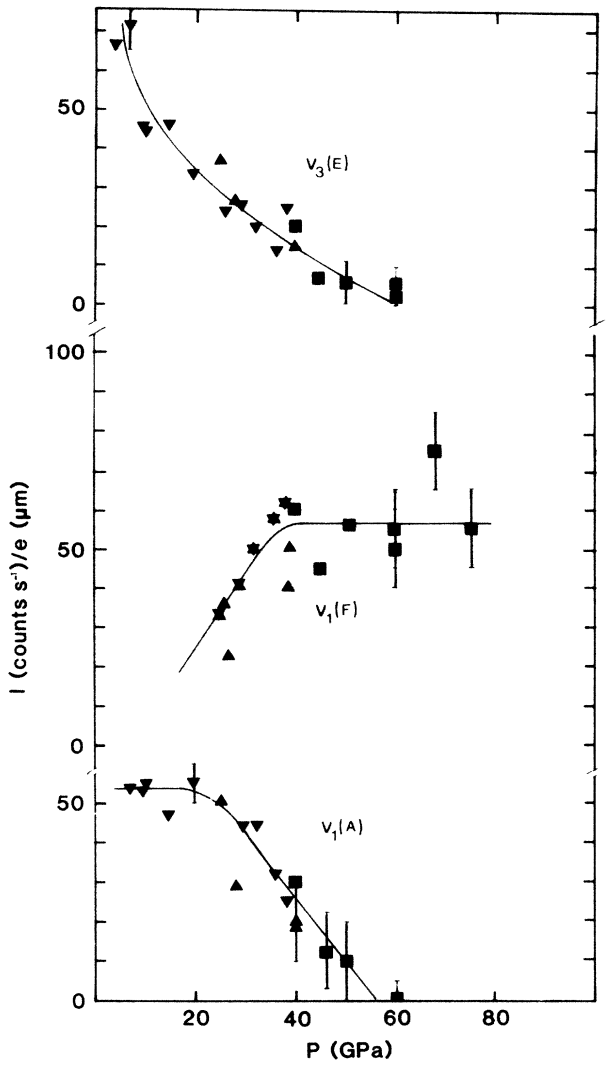

FIG. 5. Intensity (in counts/s) of the internal modes ν_1 (A), ν_1 (F), and ν_3 (E) per unit sample thickness as a function of pressure. Symbols indicate different samples; solid line, manual fit. Rough estimates of the sample thickness were provided from the NH_3 EOS (Sec. IV B) and measurements of the hole gasket diameter.

transformation involves a slight modification of structure. A marked jump in the Brillouin shift around 15 GPa, observed in this group, indicates, however, a first-order phase transition.[26] Although the birefringence pattern evolves across the transition, change in the birefringent character of the sample was not noticeable from solid phase IV to solid phase V. Grüneisen parameters are around 1.3 for the four first external modes and 0.6 for the higher-frequency rotational mode.

Beyond 14 GPa the form of the vibron bands continues to evolve strongly upon further compression. The intensity of the new band increases, whereas that of the lower-frequency component of ν_3 decreases, to disappear in the background at around 20 GPa. In the range of 14–21 GPa the envelope appears to involve six overlapping bands, whereas above 21 GPa deconvolution can be done with only four overlapping bands.

Upon further compression and in the range 30–50 GPa, the intensities of the lower frequency ν_1 and the upper frequency ν_3 decrease and the bands disappear in the background. On the other hand, the intensity of the new peak stays roughly constant (see Fig. 5).

Above 30 GPa the investigation was done with a DAC designed for very high pressure (Sec. II); the sample was too small to allow the observation of the external modes.

D. Phase VI

We have mentioned previously that above 50 GPa the spectrum around 3300 cm^{-1} only exhibits the new peak which appears at 14 GPa. A plot of ν versus p (Fig. 3) shows a discontinuity around 5 cm^{-1} close to 60 GPa. This jump is slightly above the uncertainty in this zone and suggests the occurrence of a new phase (see Secs. IV A and IV B).

IV. DISCUSSION

A. Symmetry considerations and mode assignment

In the following, starting from our Raman data, we have applied group theory to get information about crystallographic symmetries of NH_3. Description of the method can be found in the work of Decius and Hexter.[27] The notations are from the International Cristallographic Tables.[28] Prior to this discussion, symmetry properties of solid ammonia (phases I and II) at low temperature and pressure should be recalled.

1. Solid phase I

Information about solid phase I at room pressure is extensive. Its structure is $P2_13$ (T^4) with site symmetry 3 (C_3).[29,30] The unit cell contains four NH_3 molecules and consequently 16 atoms. Group-theoretical analysis assigns all 48 vibrational modes. The correlation diagram between the vibrational modes of the free molecule and the modes of the crystal is recalled[31] and completed in Table I, where we have provided the general features of the expected Raman spectra. The set of Raman-active modes consists of nine translational modes ($A+E+2F$, i.e., four Raman peaks), 12 rotational modes ($A+E+3F$, i.e., five Raman peaks), 24 internal modes, ν_1 and ν_2 of species A and F, and ν_3 and ν_4 of species E and F. It should be remembered that the (A,F) and (E,F) splittings are not due to a removal of the degeneracy but to in-phase and out-of-phase couplings between molecules of the same cristallographic cell (Davydov splitting).

From our previous analysis at 214 K,[7] and in the range 0.25–0.7 GPa, the four peaks around 3300 cm^{-1} were assigned to ν_1 (A and F), $2\nu_4$ (E), $2\nu_4$ (F), and ν_3 (E and F), respectively [Fig. 2(a)]. Low-frequency peaks are assigned to two translational bands and one broad rotational band, containing the translational and rotational modes, respectively. Other information concerning lower temperature and atmospheric pressure may be found in the literature.[21,24,25,31]

TABLE I. Symmetry species of the $k=0$ vibrations of NH_3 solid phase I $P2_13$ (T^4). T, translation; R, rotation and libration; DC, Davydov components. Raman activity in A,E,F. Infrared activity in F. Acoustic modes (translation) in F.

Molecule	Site	Crystal	Modes
C_{3v}	C_3	T	
A_1 (ν_1,ν_2)	A (R,T)	A	ν_1 (A), ν_2 (A), R (A), T (A)
		F	ν_1 (F), ν_2 (F), R (F), T (F) ν_3' (F), ν_4' (F), R' (F), T' (F) ν_3'' (F), ν_4'' (F), R'' (F), T'' (F)
E (ν_3,ν_4)	E (B,T)	E	ν_3 (E), ν_4 (E), R (E), T (E)

Line predictions

Raman lines
- 9 lattice peaks (21 modes)→4 translational peaks T ($1A+1E+2F$)
  5 rotational peaks R ($1A+1E+3F$)
- 10 internal peaks
  - 4 molecular peaks (6 modes)→ν_1 (A), ν_2 (A), ν_3 (E), ν_4 (E)
  - 6 peaks arising from phase coupling between molecules of the same cell or DC (18 modes)→ν_1 (F), ν_2 (F), ν_3' (F), ν_3'' (F), ν_4' (F), ν_4'' (F)

ir lines
- 5 lattice peaks (15 modes)→$2T$ ($2F$)+$3R$ ($3F$)
- 6 DC (18 modes)→the Raman-active components

2. *Solid phase II*

A recent neutron-diffraction investigation[4] comes to the conclusion that solid phase II, which appears above 218 K, is an hexagonal $P6_3/mmc$ (D_{6h}^4) crystal with two molecules per unit cell on site symmetry $\bar{6}m2$ (D_{3h}).

In accordance with that site symmetry, this solid is characterized by strong rotational disorder as shown by Raman scattering[7,11] and NMR.[8] Thus, correlation rules in this plastic crystal may hold only for translational modes and are likely due to librational modes (Table II). In the region of 3300 cm^{-1} the three broad peaks [Fig. 2(a)] are assigned (Table II) to internal modes ν_1 (A_1), $2\nu_4$ (E), and ν_3 (E). The two peaks ν_2 (A_1) and ν_4 (E) were observed around 1060 and 1640 cm^{-1}, respectively.[7] In the low-frequency range 100–500 cm^{-1}, two faint external modes appear and are due to translational modes T (E_{2g}) and librational modes R (E_{1g}).[7]

3. *Solid phase III*

According to the symmetry properties mentioned in Sec. III, this plastic crystal has four molecules per cell and, like solid phase II, the spectrum exhibits broad peaks. Its correlation diagram is given in Table III. Going from low to high frequencies, the different peaks of the internal spectrum [Fig. 2(b)] are assigned to ν_1 (A_1), $2\nu_4$ (E), and ν_3 (E). External modes are neither Raman nor infrared active (see Sec. III).

4. *Solid phase IV*

Above 3.8 GPa, the data on the hexagonal structure of solid ammonia are not comprehensive for the time being[1,5] (see Sec. III). Both phases II and IV have the same hcp structure.[5] Contrary to phase II, phase IV exhibits well-resolved lattice peaks above 6 GPa, which points to an ordered structure in that pressure range. Thus the site symmetry in phase IV is the free-molecule symmetry or one of its subgroups.[27] The number of the Raman-active modes then leads to the conclusion that the structure of solid phase IV is $P6_3/mmc$ (D_{6h}^4) with four molecules per unit cell on site symmetry $3m$ (C_{3v}). The proposed correlation diagram is given in Table IV. Accordingly, translational modes are of species A_{1g},E_{1g},E_{2g} and librational modes of species E_{1g} and E_{2g}. In the internal mode region and from lower frequencies, peaks are, respectively, assigned to ν_1 (A_{1g}), ν_3 (E_{2g}), and ν_3 (E_{1g}) [Fig. 2(b)].

In the range 3.8–6 GPa lattice peaks were not resolved. This is to be compared with the x-ray results concerning the c/a ratio and suggests a progressive ordering of phase IV with increasing pressure.

TABLE II. Symmetry species of the $k=0$ vibrations of NH_3 solid phase II $P6_3/mmc$ (D_{6h}^4). T, translation; R, rotation and libration. Raman activity in A_{1g},E_{1g},E_{2g}. Infrared activity in A_{2u},E_{1u}. Acoustic modes (translation) in $A_{2u}+E_{1u}$.

Molecule	Site	Crystal	Modes
C_{3v}	D_{3h}	D_{6h}	
A_1			ν_1 (A_1), ν_2 (A_1)
(ν_1,ν_2)			
E			ν_3 (E), ν_4 (E)
(ν_3,ν_4)			
	A_2'	A_{2g}	R (A_{2g})
	(R)	B_{1u}	R (B_{1u})
	A_2''	A_{2u}	T (A_{2u})
	(T)	B_{1g}	T (B_{1g})
	E''	E_{1g}	R (E_{1g})
	(R)	E_{2u}	R (E_{2u})
	E'	E_{2g}	T (E_{2g})
	(T)	E_{1u}	T (E_{1u})

Line predictions

Raman lines
2 lattice peaks (4 modes)$\rightarrow 1T$ ($1E_{2g}$)$+1R$ ($1E_{1g}$)
4 molecular peaks (6 modes)$\rightarrow\nu_1$ (A_1), ν_2 (A_1), ν_3 (E), ν_4 (E)
ir lines
4 molecular peaks (6 modes)$\rightarrow\nu_1$ (A_1), ν_2 (A_1), ν_3 (E), ν_4 (E)

TABLE III. Symmetry species of the $k=0$ vibrations of NH_3 solid phase III $Fm3m$ (O_h^5). T, translation; R, rotation and libration. Raman activity in A_{1g},E_g,F_{2g}. Infrared activity in F_{1u}. Acoustic modes (translation) in F_{1u}.

Molecule	Site	Crystal	Modes
C_{3v}	O_h	O_h	
A_1			ν_1 (A_1), ν_2 (A_1)
(ν_1,ν_2)			
E			ν_3 (E), ν_4 (E)
(ν_3,ν_4)			
	F_{1u}	F_{1u}	T (F_{1u})
	(T)		
	F_{1g}	F_{1g}	R (F_{1g})
	(R)		

Line predictions

Raman lines
4 molecular peaks (6 modes)$\rightarrow\nu_1$ (A_1), ν_2 (A_1), ν_3 (E), ν_4 (E)
ir lines
4 molecular peaks (12 modes)$\rightarrow\nu_1$ (A_1), ν_2 (A_1), ν_3 (E), ν_4 (E)

TABLE IV. Symmetry species of the $k=0$ vibrations of NH_3 solid phase IV $P6_3/mcc$ (D_{6h}^4). T, translation; R, rotation and libration; DC, Davydov components. Raman activity in A_{1g}, E_{1g}, E_{2g}. Infrared activity in A_{2u}, E_{1u}. Acoustic mode (translation) in $A_{2u}+E_{1u}$.

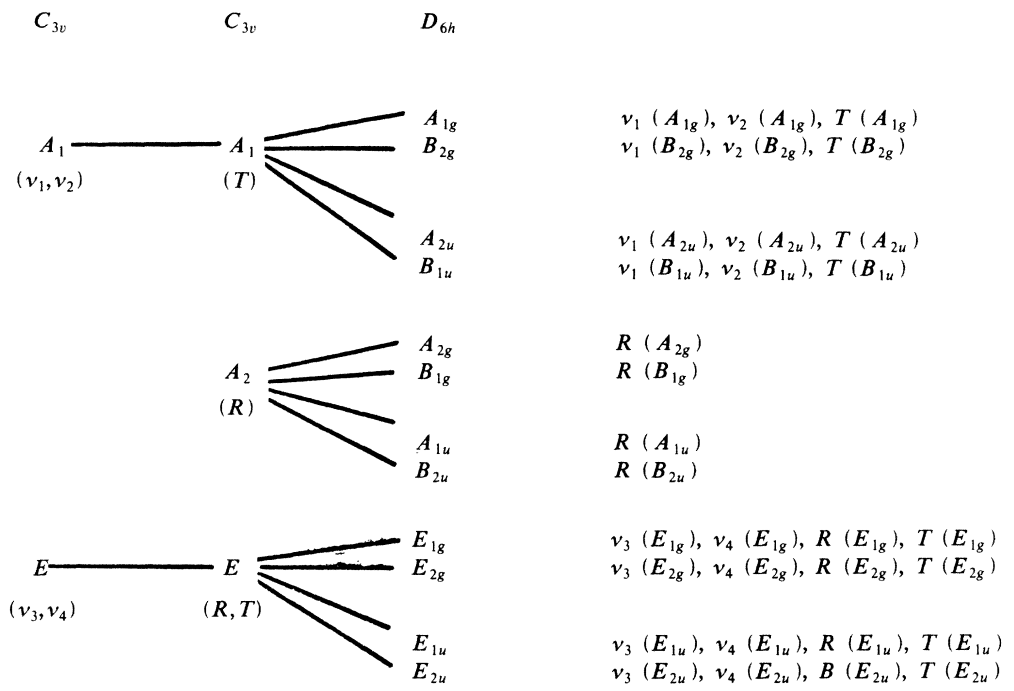

Line prediction

Raman lines
5 lattice peaks (9 modes)$\rightarrow 3T(1A_{1g}+1E_{1g}+1E_{2g})+2R(1E_{1g}+1E_{2g})$
4 molecular peaks (6 modes)$\rightarrow \nu_1\ (A_{1g})$, $\nu_2\ (A_{1g})$, $\nu_3\ (E_{1g})$, $\nu_4\ (E_{1g})$
2 DC (4 modes)$\rightarrow \nu_3\ (E_{2g})$, $\nu_4\ (E_{2g})$
ir lines
1 lattice peak (2 modes)$\rightarrow 1R(1E_{1u})$
4 DC (6 modes)$\rightarrow \nu_1\ (A_{2u})$, $\nu_2\ (A_{2u})$, $\nu_3\ (E_{1u})$, $\nu_4\ (E_{1u})$

5. *Solid phase V*

Our Raman results indicate that the transition observed around 14 GPa involves a slight structural modification (see Sec. III). It is worth noting that the extrapolation to lower pressure of frequency of the new peak, observed in the middle of the strong internal spectrum, falls within the ν_1 region at atmospheric pressure (Fig. 3). This suggests that the new frequency is a ν_1 component. Other assumptions on the nature of this new peak, such as Fermi resonance or a combination of $\nu_1\ (A)$ with a lattice mode, are less likely. The low-frequency spectrum indicates an ordered structure. Thus we can assume a $3m$ (C_{3v}) or lower site symmetry. We will consider at first $3m$ (C_{3v}) and 3 (C_3) site symmetries, then the use of the correlation tables shows that the nondegenerate vibration ν_1 is split only if the crystal structure is cubic. This involves at least four molecules per unit cell, as for solid phase I (see Sec. IV A and Table I). Among the cubic symmetries with four molecules per unit cell, only $P2_13$ (T^4) provides a plausible structure with H atoms between N atoms. The number of expected Raman-active modes is 9 (see Table I). Among structures with eight molecules per cell and $3m$ (C_{3v}) site symmetry, only $I\bar{4}3m$ (T_d^3) is possible. It has five Raman-active external modes (Table V). In the case of eight molecules per cell, we have not considered structures with 3 (C_3) site symmetry which provide either 9, 10, 11, or 12 Raman-active external modes. Some of these structures correspond to $I\bar{4}3m$ where the (110) plane is no longer a plane of symmetry for the molecule.

We have discussed the highest-symmetry structures consistent with our Raman data. Plausible lower-symmetry structures may be found among the rhombohedral group (D_{3d} and C_{3v} with C_s site symmetry). Such structures may be considered as distorted cubic structures and will not be taken into account here. We favor the simplest structures, which also provide the simplest arguments compatible with our observations.

According to what follows (see Sec. IV A) and also owing to the observed number of lattice modes, the most likely structure is $I\bar{4}3m$. The assignment of the internal and external Raman modes is given in Table V, assum-

TABLE V. Symmetry species of the $k=0$ vibrations of NH_3 solid phase V $I\bar{4}3m$ (T_d^3). T, translation; R, rotation and libration; DC, Davydov components. Raman activity in A_1,E,F_2. Infrared activity in F_2. Acoustic modes (translation) in F_2.

Molecule	Site	Crystal	Modes
C_{3v}	C_{3v}	T_d	
A_1 (ν_1,ν_2)	A_1 (T)	A_1	ν_1 (A_1), ν_2 (A_1), T (A_1)
	A_2 (R)	A_2	R (A_2)
		F_2	ν_1 (F_2), ν_2 (F_2), T' (F_2)
			ν_3 (F_2), ν_4 (F_2), R (F_2), T (F_2)
E (ν_3,ν_4)	E (R,T)	F_1	ν_3 (F_1), ν_4 (F_1), R' (F_1), T' (F_1)
			R'' (F_1)
		E	ν_3 (E), ν_4 (E), R (E), T (E)

Line predictions

Raman lines
- 5 lattice peaks (11 modes)$\rightarrow 3T(1A_1+1E+1F_2)+2R(1E+1F_2)$
- 4 molecular peaks (6 modes)$\rightarrow \nu_1$ (A_1), ν_2 (A_1), ν_3 (E), ν_4 (E)
- 4 DC (12 modes)$\rightarrow \nu_1$ (F_2), ν_2 (F_2), ν_3 (F_2), ν_4 (F_2)

ir lines
- 2 lattice peak (6 modes)$\rightarrow 1T(1F_2)+1R(1F_2)$
- 4 DC (12 modes)$\rightarrow \nu_1$ (F_2), ν_2 (F_2), ν_3 (F_2), ν_4 (F_2)

ing this structure is that of solid phase V. External modes are of species ($A_1+2E+2F_2$) and internal peaks may be, from the lower to the higher frequencies, assigned to ν_1 (A_1), ν_1 (F_2), ν_3 (F_2), and ν_3 (E) [see Figs. 2(b) and 4]. This structure is at first sight not consistent with the observed birefringence of solid phase V, which was not observed to disappear at the transition IV-V (Sec. III). However, this may not rule out our conclusion, at very high pressure birefringence being mainly due to stress inhomogeneities. The mechanism which may be invoked at the IV-V transition is rather a displacive one, often encountered from hexagonal to cubic phases. Apart from the small changes in the Raman spectrum at the IV-V transition, the slow evolution of the internal spectrum from 14 to 21 GPa and the sluggishness of the transition observed in particular during decreasing runs support that viewpoint.

6. *Solid phase VI*

From 14 GPa, the internal spectrum progressively changes to exhibit at around 50 GPa a very different form with only one peak ν_1 (F) [see Fig. 2(b)] as shown by plots of the intensity of internal vibrations ν_1 (A), ν_1 (F), and ν_3 (E) versus pressure (Fig. 5). This evolution points to modification of the nitrogen-atom environment towards a different symmetry about 50 GPa. In Sec. IV B we will interpret this in terms of possible symmetrization of the H bond at 60 GPa, where a slight jump of ν_1 (F) was observed, indicating a likely change of structure (see Sec. III). In this paragraph we will analyze the consistency of our experimental observations with that hypothesis and will discuss the possible structures of solid phase VI. Symmetrization of the H bond involves a change in the coordination number of a nitrogen atom, which should be 6 when the three initial covalent bonds and the three initial hydrogen bonds become similar with the symmetry of a regular octahedron. For that kind of symmetrized H-bonded solid the molecular concept disappears and the type of bonding compared to what is known at atmospheric pressure[32] and expected at high pressure[15,18] is ionicovalent. So the transformation at 60 GPa implies a change in the nature of the 3350-cm^{-1} peak, which would have to become a phonon mode of the lattice. Taking into account the weak mass of a hydrogen atom, this high frequency for a lattice mode is not surprising; cubic boron nitride (BN) is the closest point of comparison with NH_3 at very high pressure in regard to the individual masses of its constituents and its ionicovalent bonding. Accordingly, its bulk

modulus is 290 GPa, rather close to that expected for NH_3 at 60 GPa (240 GPa). We can then assume the force constants to be analogous in both, and taking into account the ratio of reduced masses and the value of the LO phonon in BN (1300 cm^{-1}),[33] we are led to expect a Raman mode in NH_3 around 3250 cm^{-1}, which is close to the observed value.

The internal spectrum of a system of octahedral XY_6 molecules consists mainly of one peak that arises from the totally symmetric vibration ν_1 (A_{1g}).[34] When NH_3 molecules come closer to reaching the XY_6 configuration, this vibration originates progressively from the out-of-phase coupling component ν_1 (F), which is the only peak observed above 50 GPa.

The features of the V-VI phase transformation, namely, (i) the significant change of the internal spectrum beginning well below 60 GPa and (ii) the small jump of the ν_1 (F) frequency at 60 GPa show that the structure of phase VI is closely related to that of phase V. Furthermore, the high symmetry involved by the six equivalent bonds around N atoms at the symmetrization of the H bond suggests that phase VI is very likely cubic or close to cubic.

We have accordingly searched for all cubic structures fulfilling the following properties: (i) The N-site to H-site ratio number is 3, in agreement with the ammonia formula; (ii) the nitrogen atom has six equivalent first-neighboring hydrogen atoms; (iii) the H—N—H angle is a right angle; (iv) the hydrogen atoms are at equal distances from two first nitrogen neighbors; and finally (v) the crystal is Raman active. These conditions are restrictive, and using both group-theory and x-ray cristallographic tables,[27,28] only a few structures are found. These structures pertain to two families, leading either to straight symmetric or to distorted hydrogen bonds. We will discuss only the highest-symmetry structures which characterize these two families.

7. *Pm3m* (O_h^1) *structure*

A symmetric N—H bonded ammonia solid with the simplest cubic structure $Pm3m$ may be obtained from solid phase V with structure $I\bar{4}3m$ after closure of the molecular angle H—H—H to 90° and displacement of the N atoms along the cell diagonals. Nitrogen atoms are on site symmetry $m3m$ (O_h) and hydrogen atoms on site symmetry $4/mmm$ (D_{4h}) [Fig. 6(a)]. It is to be noted that this structure is that of Cu_3N.[35] The analogy of Cu and H is not fortuitous, the structure of symmetric H-bonded ice (ice X) being that of the cuprite structure of Cu_2O.[15,17] In our case the $Pm3m$ structure is expected, owing to the directional character of the bonds.

According to Table VI the structure $Pm3m$ is not Raman active; this, however, does not rule out this structure. In fact, this structure is not dense and examination of crystal structures of compounds of the type XY_3 shows that truly cubic solids are very scarce,[35] Cu_3N being one. Generally such compounds exhibit slightly distorted cubic structures, e.g., rhombohedral or tetragonal. This may be attributed to the fact that the unstable simple-cubic nitrogen sublattice requires some distortion to be stabilized. Then, such a slight distortion for symmetric NH_3 accounts for the Raman activity. An alternative explanation might just be that stress conditions in the DAC are sufficiently inhomogeneous to lift selection rules for Raman activity.

8. *Pn3m* (O_h^4) *structure*

A $Pn3m$ structure may be obtained from solid phase V with structure $P2_13$, which may give rise only to a distorted symmetric H-bonded solid. In this case, the mechanism of the V-VI transition would involve a shift of the N atoms along diagonals of the cell and $(0,\frac{1}{2}-2x,-2x)$ directions with appropriate rotation of

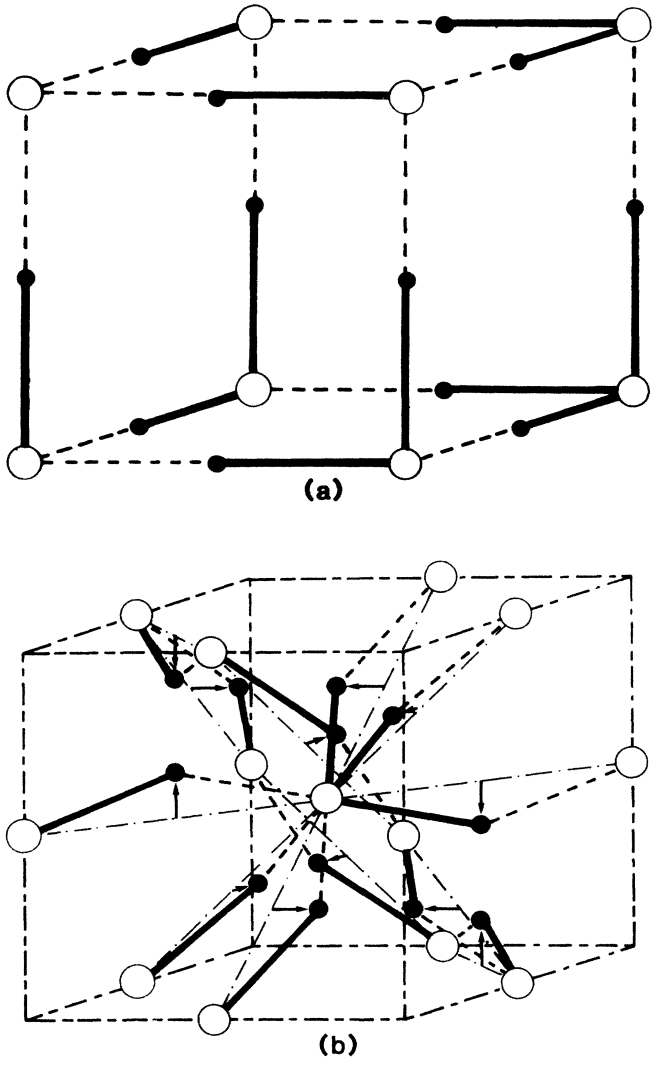

FIG. 6. Expected structure of NH_3 solid phase VI. (a) Cell of NH_3 solid phase VI $Pm3m$ (O_h^1) arising from solid phase V $I\bar{4}3m$. (b) Cell of NH_3 solid phase VI $Pn3m$ (O_h^4) arising from solid phase V $P2_13$. ○, nitrogen atoms; ●, hydrogen atoms. For clarity, the distinction is made between initial covalent bonds (——) and initial hydrogen bonds (— — —) present in phase V. Arrows in (b) indicate H positions from the middle of N-N lines.

the molecule and decrease of the H—N—H angle to 90°.

This structure has four formulas per cell. Nitrogen atoms lie on site symmetry $\bar{3}m$ (D_{3d}) and the hydrogen atoms on site symmetry mm (C_{2v}) [Fig. 6(b)]. The Raman activity involves only vibrations of the H sublattice (see Table VI). The hydrogen atoms are equidistant from two nitrogen atoms, but in contrast with the previous structures they do not lie on the N-N line connecting the nitrogen atoms. In other words, the N-H distance ($d_{\text{N-H}}$) is larger than half the N-N distance ($d_{\text{N-N}}$).

Due to the fact that distance $d_{\text{N-H}}$ is larger than $d_{\text{N-N}}/2$ and from the viewpoint of the stretching of the N-H distance (see Sec. II B), the symmetrized state is less easily obtained for this type of structure. Furthermore, symmetric bonds must be rather strong and partly ionic, consequently the N—H—N bond angle between two successive N's is rather flat. This is very likely the case for ice[15] and hydrogen halides (HBr,HCl),[36] but not for our proposed $Pn3m$ structure where the interaction angle H—N—H is close to 141°. This indicates that the most likely structure is close to $Pm3m$. On the other hand, a denser O_h^4 structure may possibly occur at higher pressure.

In conclusion, starting from solid phase V we propose two plausible families of structures. Solid phase V with structure $I\bar{4}3m$ leads to a straight symmetric H-bonded solid phase VI with structure $Pm3m$. Solid phase V with structure $P2_13$, on the other hand, leads to a distorted symmetric H-bonded solid phase VI with structure $Pn3m$.

B. Evidence for transition to a symmetric H-bonded solid

The following two main interconnected points regarding the high-pressure behavior of NH_3 will now be discussed: (i) the origin of the negative pressure shift of the

TABLE VI. Symmetry species of the $k=0$ vibrations of NH_3 solid phase VI. Raman activity in A_{1g}, E_g, F_{2g}. Infrared activity in F_{1u}. Acoustic modes (translation) in F_{1u}.

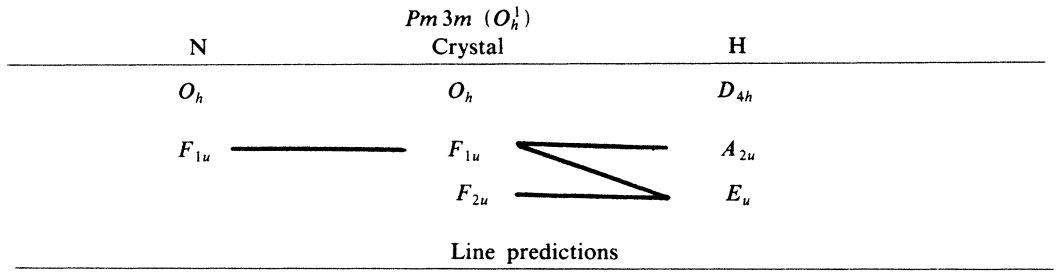

No Raman lines

ir lines

2 lattice peaks (6 modes)$\rightarrow 2F_{1u}$ (N and H sublattices)

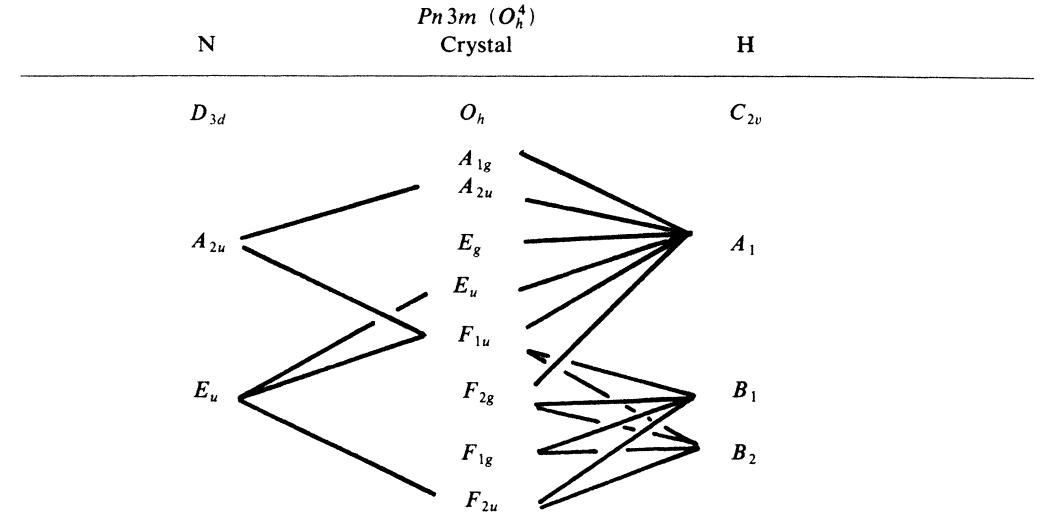

Raman lines

5 lattice peaks (12 modes)$\rightarrow 1A_{1g}$ (H) + $1E_g$ (H) + $3F_{2g}$ (H)

ir lines

4 lattice peaks (12 modes)$\rightarrow 4F_{1u}$ (N and H sublattices)

ν_1 (A) mode and (ii) the possible appearance of a symmetric H-bonded solid above 60 GPa.

It is generally observed that since atomic distances shorten with pressure, the external and internal frequencies have a positive shift up, generally to a few tens of GPa. However, in some cases, like H-bonded compounds, a reversal effect is observed as soon as density increases. Actually, it has been recognized that the covalent X-H distances of X—H $\cdots$ Y compounds, where H $\cdots$ Y is the H bond, increases with density. This is ascribed to the strengthening of the H bond, which then weakens the covalent bond and leads to a negative pressure shift of the stretching frequency. This feature is well known in water where the O-H distance in ice is larger than in the vapor phase[37,38] and is very likely the case for the N-H distance between vapor and solid ammonia.[29,30] It is clear now that such an effect may be generated by increasing the pressure, e.g., negative shift of the ν_1 and ν_3 modes of ice[15] and ν_1 mode of HBr and HCl (Ref. 36) were observed up to several tens of GPa. At atmospheric pressure, this property of the H bond has been mainly investigated for several decades by chemical physicists. Correlations were established especially between the $\nu_{X\text{-}H}$ frequency and the X $\cdots$ X distance for different X—H $\cdots$ X systems.[16,39,40]

Compared to ice, the behavior of the ν_1 and ν_3 modes of ammonia is more complicated. Its modes are split by intermolecular coupling and exhibit both positive and negative shifts. The in-phase mode ν_1 (A), which is most sensitive to the external H bond, exhibits a negative shift. The out-of-phase mode ν_1 (F), which is less sensitive to the intermolecular force, shows a positive slope. The influence of the dynamic coupling is reversed for the ν_3 modes, i.e., the ν_3 (F) component has a negative slope and the ν_3 (E) a positive slope. This behavior may be partly described using, for example, the valence force model.[34] The negative shift of ν_1 (A) and the simultaneous positive shift of ν_3 (E) of the free molecule may be ascribed to a decrease of the force constant of the N-H valence bond and an increase of the force constant of the N—N—H bond angle. Although this analysis is rather simple, it supports our hypothesis concerning the approach of a symmetric H bond which involves an increase of the N-H distance a decrease of the N—N—H molecular bond angle (Sec. IV A).

In addition to the significant changes of the internal Raman spectrum, various pieces of evidence supporting the assumption of a continuous or second-order transition to another solid state exist. It is, however, to be noted that this transition, which terminates by a jump of ν_1 (F), may be then weakly first order. This feature may be compared to what is observed at the ice-VIII–ice-X transition (the symmetric H-bonded ice).[15]

A point which supports the scheme of a continuous transition to a symmetric solid concerns the ν_1 (A) intensity. Starting from symmetry arguments (see Sec. IV A) it is clear that the ν_1 (A) mode, which corresponds to an out-of-phase motion between internal and external bonds, leads, at the symmetrization, to a Raman-inactive mode, the frequency of which should decrease as intermolecular and intramolecular forces become similar (see below). We have mentioned above that from 30 GPa the intensity of ν_1 (A) indeed progressively vanishes (see Sec. IV A and Fig. 5) and its frequency decreases. This is also the case for the ν_3 (E) mode. The second point concerns the behavior of frequency ν_1 (A) versus molar volume or $d_{N\text{-}N}$ distance. In the liquid state $d_{N\text{-}N}$ was estimated from volume data at 300 K.[3] In the solid state and below 6 GPa, molar volume and, consequently, $d_{N\text{-}N}$ were obtained from the recent x-ray data of Mills.[5] These data were fitted using an isothermal path equation where the volume jump at the transition III-IV has been taken into account. Above 6 GPa, $d_{N\text{-}N}$ could be obtained by extrapolation of that equation which fits solid phase IV. Because our extrapolation concerns pressures much higher than a few GPa we did a careful analysis with different types of equations of states. We finally chose the equation of Vinet *et al.*,[41] which has been shown to be better suited to the high-pressure range, i.e., to large volume variations, than the Murnaghan equation. The two parameters, bulk modulus and its first derivative at zero pressure are found to be 3.7 GPa and 5.65, respectively. The frequency ν_1 (A) versus $d_{N\text{-}N}$, computed as indicated above, is plotted in Fig. 7. The plot exhibits a nonlinear behavior for $d_{N\text{-}N}$ below 2.9 Å, that is, around 20 GPa. Extrapolation points to a rapid decrease for $d_{N\text{-}N}$ in the 2.6–2.7 Å range or according to our equation of state close to 60 GPa. This pressure zone is close to the point where we have observed a jump of ν_1 (F). The estimation of $d_{N\text{-}N}$ at pressure as high as several tens of GPa is very crude and the above correlation may be fortuitous. However, if we rely upon the validity of high-pressure equations of state, such as those used here (Murnaghan or Vinet), the relative accuracy of $d_{N\text{-}N}$ may be estimat-

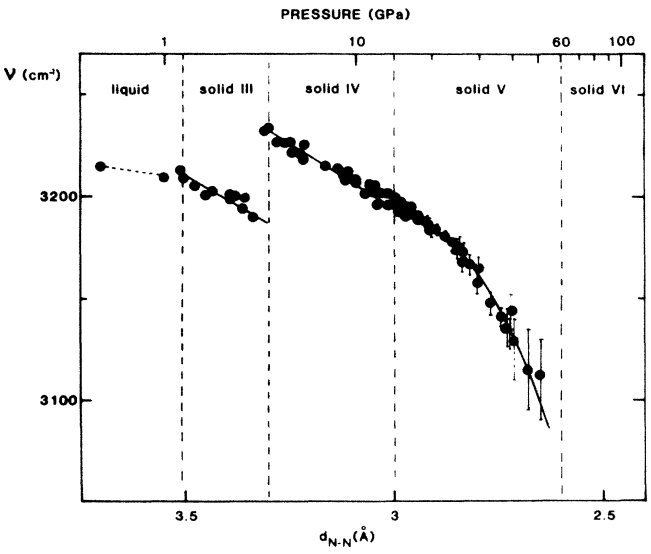

FIG. 7. Frequency ν_1 (A) as a function of estimated distance $d_{N\text{-}N}$. Distance $d_{N\text{-}N}$ is provided by the NH_3 EOS (Sec. IV B). Solid curve, manual fit; dashed lines, phase transformation locations.

ed to be better than 4%. The corresponding pressure margin is roughly ±15 GPa around 60 GPa. It is to be noted here that we were not able to take into account the effects due to the IV-V transition, which very likely involve a small volume jump and weak changes on the parameters of our equation.

An estimate of the $d_{N\text{-}N}$ distance for a symmetric H bond may be obtained from the physicochemical studies mentioned above. Correlations have been established between quantities such as $\nu_{X\text{-}H}$, $d_{X\text{-}H}$, and $d_{X\text{-}X}$,[16,40] although such correlations are well known only for the (O-O,O-H) pair. A crude comparison between the variations of $\nu_{X\text{-}H}$ versus $d_{X\text{-}X}$ between the O—H $\cdots$ O and N—H $\cdots$ N systems gives an upper limit of 2.7 Å for $d_{N\text{-}N}$ when symmetrization occurs. This is supported by a recent infrared band-shape analysis in imidazol crystals at low temperature, which indicates that the N-N distance for N—H $\cdots$ N symmetric systems must lie between 2.65 and 2.75 Å.[42]

It is, however, of interest to note that the $\nu_{N\text{-}H}$ versus $d_{N\text{-}N}$ variation observed in nitrogen compounds at room pressure[40] is quite different from that obtained in the present work (Fig. 7). Indeed, in the range of 3.3–2.7 Å for $d_{N\text{-}N}$, we obtain an average slope $d\nu_{N\text{-}H}/d(d_{N\text{-}N})$, which is nearly one order of magnitude less than the slope obtained from data at ambient pressure. Comparison of results concerning H_2O and O—H $\cdots$ O systems leads to a less marked difference. In contrast to H_2O, the molecular angle H—X—H in NH_3 undergoes a large change from 107° to 90° under pressure and this alone would account for the difference between the two systems. Moreover, variations such as $\nu_{X\text{-}H}$ versus $d_{X\text{-}X}$ obtained from physicochemical and high-pressure studies are not expected to be the same since the charge transfer mechanism versus $d_{X\text{-}H}$ is different.

A point which is relevant to that comparison concerns the value of $\nu_{X\text{-}H}$ in the symmetrized state. Physicochemical papers provide values for $\nu_{O\text{-}H}$ and $\nu_{N\text{-}H}$ slightly below 1000 cm^{-1}.[40] In both high-pressure investigations of NH_3 and H_2O, ν_1 peaks were observed to disappear in the background 10 or 20 GPa from the expected symmetrization pressure p_s, so it was not possible to measure the trend close to the symmetrized state. However, it is possible to provide an estimate for the limit of $\nu_{N\text{-}H}$, which in fact is found to lie above 1000 cm^{-1}. We have previously mentioned the change in the nature of the ν_1 (F) mode when solid phase V transforms to solid phase VI; this obviously holds for the ν_1 (A) mode. We will use hereafter a linear chain model similar to that proposed by Zallen.[43] We start with two atoms per unit cell and two force constants $k_{N\text{-}H}$ and $k_{H\cdots N}$ for the covalent bond and the H bond, respectively. Modes ν_1 (A) and ν_1 (F) pertain to the same phonon dispersion branch and, due to the respective motions involved, $\nu_1(A)$ is a zone-center mode and ν_1 (F) a zone-boundary mode. In the ν_1 (A) mode the external bond vibrates out of phase with the internal bond and the external-bond constants contribute to the restoring force. It is worth noting that this model predicts a ν_1 (A) frequency higher than ν_1 (F). In fact, in this model only first-neighbor interactions are considered, whereas longer-range interactions should be taken into account. In an actual solid with $Pm3m$ structure, H atoms are surrounded by eight H nearest neighbors and H-H interaction must play a large role. Furthermore, it is agreed that many-body effects play a significant role in the free energy of molecular solids, especially those with anisotropic molecules. This remark is very likely relevant to H-bonded solids. Besides, as is expected at high pressure, interactions must concern a range spreading out beyond the first neighbors. Using again the linear chain model, a longer-range interaction may be simulated by adding two positive force constants k_N and k_H between N atoms and H atoms, respectively. This model leads for a symmetric H-bonded chain ($k_{N\text{—}H}=k_{H\cdots N}=k_s$) to the characteristic frequencies

$$\omega_1=[2(k_s+k_H)/m_N]^{1/2} \tag{1}$$

for the zone-boundary acoustic mode,

$$\omega_0=(2k_s/\mu)^{1/2} \tag{2}$$

for the zone-center optical mode, and

$$\omega_0'=[2(k_s+k_H)/m_H]^{1/2} \tag{3}$$

for the zone-boundary optical mode, where we have assumed for simplicity $k_N=k_H$, which is quite reasonable if only electrostatic forces and mass ratio are taken into account and where m_H and m_N are, respectively, H and N masses, and μ the corresponding reduced mass. With $k_H=0$, Eqs. (1)–(3) lead to the well-known equations for a diatomic chain. The unit cell may then be doubled, introducing, for example, a slight difference between alternating k_s.[43] This first accounts for the correlation field splitting (Davydov doublet), which gives two high external frequency branches and secondly provides a low-frequency optical branch. According to our model, ω_0 and ω_0', which may be larger than ω_0, correspond to ν_1 (A) and ν_1 (F), respectively. Using our data, i.e., ν_1 (F) = 3340 cm^{-1} at p_s, Eq. (3) gives k_s+k_H. This allows us to estimate the lower-frequency optical mode, which is found close to 900 cm^{-1}; this is in accordance with the extrapolation to 60 GPa of the ν_T frequencies in Fig. 4. Now assuming $k_s=k_H$, a lower value at around 2340 cm^{-1} for the ν_1 (A) frequency is obtained through Eqs. (1) and (2). It is of interest to note that for ν_1 (A) = 3000 cm^{-1}, which is the extrapolated value from Figs. 3 and 7, the ratio k_H/k_s obtained from Eqs. (2) and (3) is around 0.3. Actually, for a real solid, this ratio is expected to be slightly smaller. In fact, in a three-dimensional model, k_H results from the H-H nearest-neighbor interactions and the amount of such interactions is larger than that of N-H interactions. This simple formal model indicates a ν_1 (A) value at p_s, which is clearly above the physicochemical data but in better agreement with our results. A more elaborated model is required to have a better understanding about the pressure dependence of ν_1 (A) and ν_1 (F) and the evolution of the H bonding.

V. CONCLUSION

Within the resolution of our Raman scattering investigation, some significant features of the phase diagram of NH_3 have been determined at room temperature up to 75 GPa.

Solid phase III, in accordance with previous data, is found to be fcc. Its space group is $Fm3m$ (O_h^5) with site symmetry $m3m$ (O_h). This phase is a disordered solid.

Solid phase IV, which occurs at 3.8 GPa, has, in accord with x-ray data,[5] space group $P6_3/mmc$ (D_{6h}^4); above 6 GPa the site symmetry is found to be $3m$ (C_{3v}). Solid phase V, which appears at 14 GPa, is very likely cubic, and a $I\bar{4}3m$ (T_d^3) structure with site symmetry $3m$ (C_{3v}) would fit our data.

Around 60 GPa solid phase V transforms to solid phase VI, also cubic or close to cubic, and a plausible structure is $Pm3m$ (O_h^{-1}), with a slight distortion, N atoms being on site symmetry $m3m$ (O_h), H atoms on site symmetry $4/mmm$ (D_{4h}).

It is clear from Tables I–III that with increasing temperature the molecular centers shift to sites of higher symmetry, indicating the onset of molecular rotational disorder. This step is achieved along the sequence I-II-III. On the other hand, with increasing pressure, Tables III and IV show that the site symmetry shifts towards $3m$, the molecular symmetry. This step is reached at the end of the sequence of transition III-IV (at 6 GPa). It corresponds to the vanishing of the molecular rotational disorder. On further compression, our results show a shift of the symmetry around N atoms towards higher symmetry. This process, which begins around 20 GPa, corresponds to a progressive change in the nature of the intermolecular and the chemical covalent bonds. This assumption is mainly supported by the significant change of the internal spectrum, the strong decrease of the Raman intensity of the intramolecular mode ν_1 (A), and its negative pressure shifts, which mainly occurs along the sequence V-VI. We conclude that this process, which leads to disappearance of the molecular character, is reached around 60 GPa where symmetric bonding occurs. Infrared spectroscopy and x-ray diffraction investigations are required to get firm conclusions about structures of solid phases V and VI.

ACKNOWLEDGMENTS

We are indebted to Dr. R. L. Mills for communicating his preliminary x-ray results on ammonia solid phase IV. Helpful discussions with Dr. F. Fillaux, Dr. A. Polian, Dr. P. Loubeyre, and Dr. M. Krauzman are acknowledged. We are also grateful to Dr. W. Holzapfel and Dr. P. Johannsen for stimulating discussions and relevant comments. The Physique des Milieux Condensés is Unité Associée au Centre National de la Recherche Scientifique No. UA 782.

[1]R. C. Hanson and M. Jordan, J. Phys. Chem. **84**, 1173 (1980).

[2]R. B. Von Dreele and R. C. Hanson, Acta Crystallogr. Sect. C **40**, 1635 (1986).

[3]R. L. Mills, D. H. Liebenberg, and Ph. Pruzan, J. Phys. Chem. **86**, 5219 (1982); R. L. Mills, D. H. Liebenberg, A. Le Sar, and Ph. Pruzan, *Proceedings of the Materials Research Society Symposium,* edited by C. Homan, R. K. Mac Crone, and E. Whalley (North-Holland, Amsterdam, 1984), Vol. 22, p. 43.

[4]J. Eckert, R. L. Mills, and S. K. Satija, J. Chem. Phys. **81**, 6034 (1984).

[5]R. L. Mills (private communication).

[6]C. L. Nye and F. D. Medina, Phys. Rev. B **32**, 2510 (1985).

[7]M. Gauthier, Ph. Pruzan, J. M. Besson, G. Hamel, and G. Syfosse, Proceedings of the Tenth AIRAPT Conference, edited by N. J. Trappeniers, S. N. Biswas, H. R. van der Berg, C. Prins, K. O. Prins, and J. A. Schouten (Amsterdam, July 1985), [Physica B **139/140**, 218 (1986)].

[8]M. A. Doverpike, S. B. Liu, P. Ennis, T. Johnson, M. S. Conradi, K. Luszczynski, and R. E. Norberg, Phys. Rev. B **33**, 14 (1986).

[9]H. Kiefte, S. W. Brecken, R. Penney, and M. Clouter, J. Chem. Phys. **83**, 4738 (1985).

[10]R. C. Hanson (unpublished).

[11]R. K. Luo, C. Nye, and D. Medina, J. Chem. Phys. **85**, 4903 (1986).

[12]W. B. Holzapfel, R. S. Hawke, and K. Syassen, in *Proceedings of the Fourth International Conference on High Pressure,* edited by J. Osugi, K. Suzuki, M. Koizumi, T. Makita, and S. Matsushima (Physico-Chemical Society of Japan, Kyoto, 1975), p. 344.

[13]G. E. Walrafen, M. Abebe, F. A. Mauer, S. Block, G. J. Piermarini, and R. G. Munro, J. Chem. Phys. **77**, 2166 (1982).

[14]G. P. Johari and H. A. M. Chew, Philos. Mag. B **49**, 647 (1984).

[15]K. R. Hirsch and W. B. Holzapfel, Phys. Lett. A **101**, 142 (1984); J. Chem. Phys. **84**, 2771 (1986), and references therein.

[16]I. Olovsson and P.-G. Jonsson, in *The Hydrogen Bond, Structure and Spectroscopy,* edited by P. Schuster, G. Zundel, and C. Sandorfy (North-Holland, Amsterdam, 1976), Vol. II, p. 393.

[17]A. Polian and M. Grimsditch, Phys. Rev. Lett. **52**, 1312 (1984); A. Polian, J. M. Besson, and M. Grimsditch, in *Solid State Under Pressure,* edited by S. Minomura (KTK Scientific Publishers, Tokyo, 1985), p. 93.

[18]K. S. Schweizer and F. H. Stillinger, J. Chem. Phys. **80**, 1230 (1984).

[19]For a survey on this technique, see A. Jayaraman, Rev. Mod. Phys. **55**, 65 (1983); Rev. Sci. Instrum. **57**, 1013 (1986).

[20]H. K. Mao, P. M. Bell, J. W. Shaner, and D. J. Steinberg, J. Appl. Phys. **49**, 3276 (1978).

[21]D. S. Binbrek and A. Anderson, Chem. Phys. Lett. **15**, 421 (1972), and references therein.

[22]J. W. Lundeen and W. H. Koehler, J. Phys. Chem. **79**, 2957 (1975).

[23]M. Buback and K. R. Schulz, J. Phys. Chem. **80**, 2478 (1976).

[24]F. P. Reding and D. F. Hornig, J. Chem. Phys. **22**, 1926 (1954).

[25]A. S. Pine, C. J. Glasbrenner, and G. Dresselhaus, *Proceedings of the International Conference on Phonons, Rennes,* edited by M. A. Nisimovici (Flammarion, Paris, 1971), p. 258.

[26]M. Gauthier, Ph. Pruzan, J. C. Chervin, and A. Polian (un-

published).
[27]J. C. Decius and R. M. Hexter, *Molecular Vibrations in Crystals* (McGraw-Hill, New York, 1976).
[28]*International Tables for X-Ray Cristallography,* edited by N. F. M. Henry and K. Lonsdale (Kynoch, Birmingham, England, 1965).
[29]I. Olovsson and D. H. Templeton, Acta Crystallogr. **12**, 832 (1954).
[30]J. W. Reed and P. M. Harris, J. Chem. Phys. **35**, 1730 (1961).
[31]F. P. Redig and D. F. Hornig, J. Chem. Phys. **19**, 594 (1951).
[32]Y. Matsui, K. Ezumi, and K. Iuatani, J. Chem. Phys. **84**, 4774 (1986), and references therein.
[33]J. A. Sanjurjo, E. Lopez-Cruz, P. Vogl, and M. Cardona, Phys. Rev. B **28**, 4579 (1983).
[34]G. Herzberg, *Molecular Spectra and Molecular Structure* (Van Nostrand, New York, 1945), Vol. II.
[35]R. W. G. Wyckoff, *Crystal Structures,* 2nd ed. (R. E. Krieger, Malabar, FL, 1986), p. 45.
[36]R. A. Noak and W. B. Holzapfel, in *High Pressure Science and Technology,* Proceedings of the Sixth AIRAPT Conference (Boulder, 1977), edited by K. D. Timmerhaus and M. S. Barber (Plenum, New York, 1979), Vol. 1, p. 748; P. G. Johansen, W. Helle, and W. B. Holzapfel, XXIInd Meeting of the EHPRG (Aussois, 1984) [J. Phys. (Paris) Colloq. Suppl. **11**, C8-199 (1984)].
[37]D. Eisenberg and W. Kauzman, *The Structure and Properties of Water* (Oxford, London, 1969).
[38]E. Whalley and D. D. Klug, J. Chem. Phys. **84**, 78 (1986), and references therein.
[39]S. Walker and H. Straw, *Spectroscopy* (Chapman and Hall, London, 1962), Vol. 2, p. 177.
[40]A. Novak, in *Structure and Bonding,* edited by J. H. Fuhrhop, G. Blauer, T. J. R. Weakley, and A. Novak (Springer, Berlin, 1974), Vol. 18, p. 177.
[41]P. Vinet, J. Ferrante, J. R. Smith, and J. H. Rose, J. Phys. C **19**, L467 (1986).
[42]F. Fillaux (unpublished).
[43]See, e.g., W. F. Sherman and G. R. Wilkinson, in *Advances in Infrared and Raman Spectroscopy,* edited by R. J. H. Clark and R. H. Hester (Heyden, London, 1980), Vol. 6, p. 158.